JES
Journal of Engineering Sciences
Vol 11, Issue 3, MARCH /2020
ISSN NO:0377-9254

TRANSFORMERLESS PHOTOVOLTAIC GRID-CONNECTED INVERTERS FOR SOFT-SWITCHING CONFIGURATION AND ITS APPLICATION

1N.AHMED HUSSAIN, 2S.SASIDHAR REDDY, 3M.NAVEEN BABU
1M.Tech Student, 2,3Asst.Professor
Department Of Electrical Electronics Engneering
Tadipatri Engneering College, Tadipatri

Abstract— Soft-switching techniques of transformerless photovoltaic grid-connected inverters (TLI) can significantly reduce switching losses, as well as soften switching processes. Conventional DC-AC soft-switching configurations proposed by Dr. Divan are invalid in TLIs because of leakage current problem (LC). In order to develop soft-switching techniques in TLIs, this paper proposes a new soft-switching configuration and a procedure to guide the invention of soft-switching TLIs. First, this paper proposes two basic resonance tanks related to DC bus polarities; then uses these basic tanks to elevate four popular full bridge type TLIs according to the proposed guideline. As a result, four soft-switching TLIs are gained. Second, this paper picks obtained soft-switching highly efficient and reliable inverter concept (HERIC) as example to analyze its soft-switching operation principle and performance. As a consequence, all active switches of the gained soft-switching HERIC circuit are switched under both of zero-current turn-on and turn-off conditions; the reverse recovery problem of freewheeling diodes is alleviated owing to the zero-current turn-off of diodes; meanwhile, the common-mode voltage at the switching frequency scale is still constant. Finally, some experimental results from a 3-kW universal prototype at 50-kHz switching frequency are provided to verify the effectiveness of main contributions of this paper.

Index Terms—Soft-switching configuration, Basic resonance tank, Transformerless PV Grid-connected inverter.

I. INTRODUCTION

Transformerless grid-connected inverter (TLI) topologies have become a widespread tendency in low power distributed photovoltaic (PV) generation systems [1-8], such as HERIC [9], H5 [10], and H6s [11-13], etc., for they feature simple circuit structure, low cost, and high reliability. In practice, their switching frequency has been chosen in 10-20 kHz range in order to maintain higher efficiency

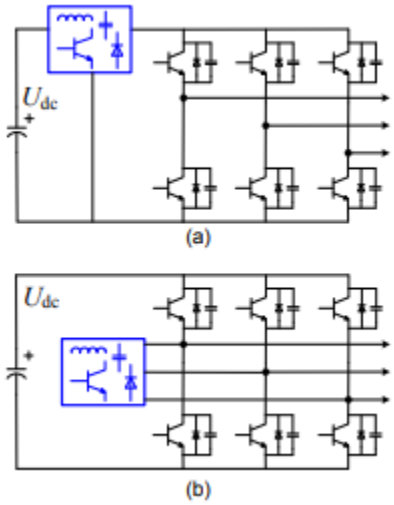

Fig. 1. Conventional Soft-switching configurations for DC-AC inverters. (a) DC-side configuration. (b) AC-side configuration

(forexample, more than 98%) [14, 15]. As a consequence, the size and weight of present TLIs are difficult to be cut down further, and their power density is much lower than the state-of-the art of DC-DC converters [16-18]. Using wide bandgap (WBD) devices in TLIs is an effective means to raise the switching frequency and power density. That is, therefore, recognized as one of essential techniques for next-generation PV grid-connected inverters [19]. However, some challenges, such as switch ringing and switching stresses of WBDs, must be overcome. Otherwise, they would jeopardize the reliability and electromagnetic compatibility (EMC) of WBD-TLIs [20]. Referring to the truth that soft-switching techniques take the role in the development of DC-DC converters, it is still an option for TLIs. The soft-switching technique is able to not only reduce switching losses for silicon-based TLIs but also overcome the switching ringing and switching stresses for WBD-TLIs. Generally, there are some merits for TLIs with soft-switching techniques, for instance, 1) the TLIs might get rid of the constraint of switching frequency because of less switching loss; 2) since the rising and falling processes of power semiconductor devices are softened, the problems of switch ringing and switching stresses of WBDs could

be overcome; 3) the layout of high frequency circuits would be getting easier as parasitic parameters could be treated as resonant components [21]. In the past decades, there had been many studies on soft-switching techniques for DC-AC inverters. In general, those soft-switching topologies can be classified into two categories: DC-side and AC-side soft-switching circuits [22], according to positions where the resonance tanks are located at. The detailed configurations are shown in Fig. 1 (a) and (b), also known as resonant DC link inverters [23], and resonant pole inverters [24], respectively. In Fig. 1(a), one inductor and one capacitor are inserted between the DC source and the inverter bridge by Dr. Divan at the beginning. The circuit structure is simple, but it imposes substantial voltage stress (more than 2.5 times the DC input voltage) across the power semiconductor devices, and the resonant tank carries the full load current at least. Although subsequently improved circuits lowered the voltage stress, the problem of the conduction loss in resonant tanks still limits its application in practice. In Fig. 1 (b), the resonant tanks are shifted to a parallel-position from the series-position of Fig. 1 (a), and it is a significant improvement. Meanwhile, the voltage stress of devices is clamped on the DC input voltage. However, the conduction loss of resonant inductors is still unacceptable, and the current stress of bridge switches is significantly increased as well. In theory, such two categories of soft-switching configurations could be directly used in isolated PV grid-connected inverters with either high-frequency or line-frequency transformer. Unfortunately, they could not be used in TLIs because of leakage current problem [27-29]. Therefore, TLIs need a new soft-switching configuration taking into account the common-mode voltage (CMV) performance. Some researchers have tried soft-switching techniques for TLIs. Gekeler proposed a soft switching three-level inverter with a passive snubber circuit [25-26], named as S3L inverter. As a result, the switching losses in switches and diodes have been reduced by just using few passive components. Unfortunately, the two-level output differential-mode voltage (DMV) appears in the commutating period in order to make the resonant inductor reset. Obviously, the added snubber circuit worsens the DMV and CMV performance. Xiao et al. proposed a series of soft-switching TLIs. First, literature [27] introduces zero-voltage transition (ZVT) tanks into H6-I. As a result, the ZVS for main switches and ZCS turn-on for added auxiliary switches are obtained. Subsequently, ZVT tanks are successfully introduced into HERIC in [28], which means that the soft-switching technique has been fulfilled based on the best TLI topology because HERIC has the minimum conduction loss in all TLIs so far. Unfortunately, the turn-off loss of added auxiliary switches still exists in [28]. In duality, literature [29] realizes zero-current transition (ZCT) function based on H6-I, but the losses including main switches' turn-on, added auxiliary switches' turn-off, and diodes' reverse recovery are still remained in ZCT- H6-I. According to the aforementioned review and comments, there are two urgent tasks to keep studying for soft switching TLIs. First, a distinct soft-switching configuration concerning TLIs' property is necessary in order to guide the invention of soft-switching topologies. The second one is about switching loss, i.e., how to lower the total switching loss to the least, especially for HERIC.

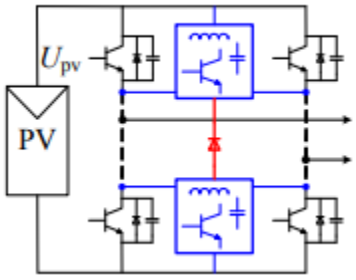

Fig2: New soft-switching configuration for TLIs.

The major contributions of this paper are to propose a new soft-switching configuration for TLIs, as well as to use it in creating soft-switching TLIs with the smallest switching loss.

II.PHOTOVOLTAIC INVERTER

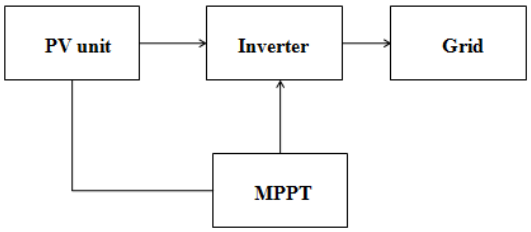

Fig3. Schematic diagram of PV system

The AC power delivered from the inverter is given to the grid for the power generation. The specifications of grid are given in Table 3.4.

Analytical models are essential in the dynamic performance, robustness, and stability analysis of different control strategies. To investigate these features on a three phase grid connected PV system, the mathematical model of the system needs to be derived. The modeling of the proposed system includes:

1. Photovoltaic cell and PV array modeling
2. Three phase inverter model
3. Three phase fundamental transformations modeling

In this chapter, the operation and role of each of these components will be described and their mathematical model will be derived.

3.1.1 Photovoltaic cell and array modeling

A PV cell is a simple p-n junction diode that converts the irradiation into electricity. Fig.3.2 illustrates a simple equivalent circuit diagram of a PV cell. This model consists of a current source which represents the generated current from PV cell, a diode in parallel with the current source, a shunt resistance, and a series resistance.

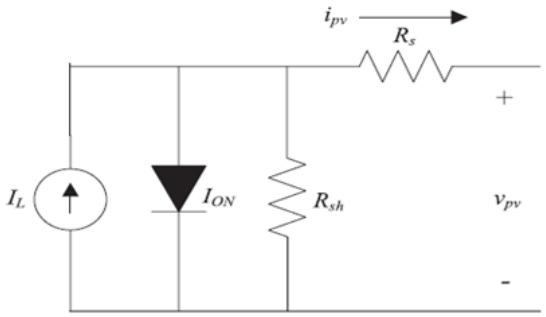

Fig4. Equivalent circuit diagram of the PV cell

III.OPERATION AND CONTROL DESIGN NEW SOFT-SWITCHING CONFIGURATION FOR TLIS

A. Soft-switching configuration

Since two conventional soft-switching configurations can not be used in TLIs, a new soft-switching configuration fitting for TLIs is necessary. Fortunately, TLIs do provide an opportunity for creating the new soft-switching configuration, for they have dedicated zero-vector freewheeling branches. This paper has successfully proposed a new soft-switching configuration based on the zero-vector freewheeling path, which is illustrated in Fig. 2. There are some distinct features in comparing with Fig. 1 (a) and (b). First of all, there are two tanks with different DC bus polarities. Therein, the top tank is named as positive Bus-tank, and the bottom one is named as negative Bus-tank, respectively. Second of all, two tanks are in parallel with the power flow loop of TLIs, and both of them have the connections with DC bus and AC side at the same time. The last and most important, there is a freewheeling branch connected between two tanks. It is worth noting that the freewheeling branch is not only for freewheeling loop at the zero-vector stage but also for resonance tanks resetting. From the perspective of operation principle, there are several differences with Fig. 1 as well. 1) In Fig. 1 (a), all bridge switches share one resonance tank, and its modulation strategy is limited by many restrictions, yet two switches in one bridge leg share a part of resonance tanks in Fig. 1 (b). In Fig. 2, however, two switches with the same bus polarity share one complete resonance tank. 2) At the power handling stage, two resonance tanks of Fig. 2 are separated in order to create independent soft-switching moment for each of high-frequency switches; then, two resonance tanks are linked each other to synchronize with AC output filter at the free wheeling stage.

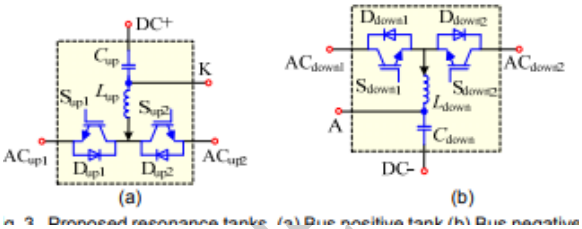

Fig5: Proposed resonance tanks. (a) Bus positive tank (b) Bus negative tank

B. Basic resonance tank

This paper also creates two resonance tank circuits to fit Fig. 2, and they are shown in Fig. 3 (a) and (b), respectively. In Fig. 3 (a), Bus positive tank includes resonant switch Sup1 with diode Dup1, resonant switch Sup2 with diode Dup2, resonant inductor Lup, and resonant capacitor Cup. Particularly, one terminal of resonant capacitor Cup is connected with the bus positive polarity; the emitters of Sup1 and Sup2 are connected to AC terminals ACup1 and ACup2, respectively; the midpoint K is allocated to connect with the cathode of the diode freewheeling loop. In duality, Bus Negative tank composed of resonant switch Sdown1 with diode Ddown1, resonant switch Sdown2 with diode Ddown2, resonant inductor Ldown, and resonant capacitor Cdown is illustrated in Fig. 3 (b). Similarly, one terminal of resonant capacitor Cdown is connected with the bus negative end; the collectors of Sdown1 and Sdown2 are connected to AC nodes ACdown1 and ACdown2, respectively; the midpoint A is appointed to connect with the anode of the diode freewheeling loop.

C. Using the soft-switching configuration and basic resonance tanks in TLIs

High efficiency and low leakage current (LC) are two key indexes for TLIs. Using proposed soft-switching configuration might improve the efficiency of TLIs as discussed in Introduction. However, the LC is a mandatory item by Standards, such as VDE 0126-1-1, which implies that all TLIs, that want to be sold on the market, must comply with. Xiao and Xie concluded an evaluating guidance of the LC for the bridge type TLIs in [30]. The conclusion is that the LC depends on the amplitude and frequency of the CMV under the condition of that two filter inductors are symmetrically placed in phase line and neutral

line, respectively. In brief, the constant CMV induces no LC. Later on, a diode clamping strategy at the freewheeling stage had been proposed by Xiao and Xie in [31], which is an efficient means to maintain the CMV constant in whole switching period [3, 6]. In order to follow the LC standards and keep the LC at the lowest level, this paper introduces the diode clamping approach into the proposed soft-switching configuration to replace the previous single diode freewheeling in Fig. 2. Based on aforementioned resonance tanks and rules, four popular TLIs with soft-switching functions and CVM clamping are gained,

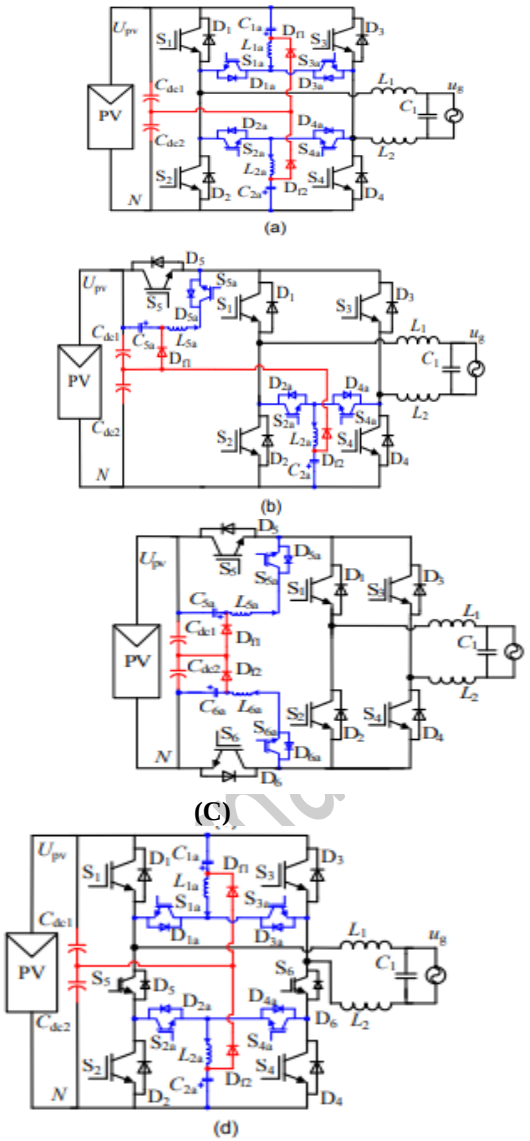

Fig6: A family of SLF-SLIs. (a) SLF-HERIC. (b) SLF-H5. (c) SLF-H6-I. (d) SLF-H6-II.

and they are shown in Fig. 4 (a), (b), (c), and (d), respectively. In order to keep the name consistent with the former hard-switching TLIs, the gained topologies are named as SLF-HERIC, SLF-H5, SLF-H6-I, and SLF-H6-II, respectively. Here, the abbreviation 'SLF' means switching loss-free, which is going to be explained in detail in the next section. Another one is also worth noting that in SLF-H5 and SLF-H6-I, there are half Bus tanks fitted for switch S5 and S6. The reason is that S5 and S6 are shifted into DC buses. As a result, one of resonant switches is cut down in half Bus resonance tanks.

IV.OPERATION PRINCIPLE ANALYSIS BASED ON SLF-HERIC

This section picks SLF-HERIC to discuss its operation principle. For the sake of analysis, the CMV clamping branch is removed first, since the operation principles of the resonance tanks and the CMV clamping branch can be separately discussed. The simplified SLF-HERIC is illustrated in Fig. 5(a), Bus positive tank involves resonant components C1a, L1a, and auxiliary switches S1a, S3a; and Bus negative tank is composed of resonant components C2a, L2a, and auxiliary switches S2a, S4a. Meanwhile, L1a=L2a=Lr and C1a=C2a=Cr; Df is the freewheeling diode. Switches S1-S4 are the high frequency main switches, and an ideal alternating current source represents the output AC filter and grid. The driving signals of SLF-HERIC with unity power factor are shown in Fig. 5(b) (at the grid-frequency-scale, the dimensions of some signals may be exaggerated for the sake of simplicity and clarity of illustration). In the positive half period of grid, S1 and S4 have the same driving signal; in the negative half period, S2 and S3 have the same driving signal. In addition, the gating signals of S1a and S4a accompanying S1 and S4 are enabled in the positive half period; similarly, the gating signals of S2a and S3a fallowing S2 and S3 are acted in the negative half period. It can be seen from Fig. 5(b), the duty cycle of high frequency main switches is denoted as D1; the duty cycle of auxiliary switches is marked with D2. There are two overlapping time zones, one is $_{DA}1$ at the end of high frequency switches' pulse; another one is $_{DA}2$ at the beginning of high frequency switches' pulse. There are nine stages in one switching period, and the key operation waveforms of SLF-HERIC in the grid current positive half cycle are illustrated in Fig. 5(c). The corresponding equivalent circuits for each stage are illustrated in Fig. 6. Stage 1 [t0, t1]: Before t0, S1 and S4 are on, and it is at the normal power handling stage like hard-switching HERIC. In detail, the voltage uCa across resonant capacitors C1a, and C2a is a constant value, i.e. uC1a=uC2a=0.5UPV. The current iLa

through resonant inductors L1a and L2a is zero, i.e. iL1a=iL2a=0; the AC output current amplitude is IL. At t0, S1a and S4a are turned on, resonant capacitors start to resonate with their resonant inductors, respectively. The equivalent circuit is shown in Fig. 6(a). Currents iS1a and iS4a through the auxiliary switches and current iLa through resonant inductors rises at a sine slope from zero. As a result, the ZCS turn-on condition of auxiliary switches S1a and S4a is achieved. Meanwhile voltage uCa across resonant capacitors decreases at a cosine slope from 0.5UPV; the current through S1 and S4 begins to decrease until they equal zero at t1. At this stage,

$$i_{La}(t) = I_{La}\sin[\omega_r(t-t_0)] = i_{S1a} \quad (1)$$

$$u_{Ca}(t) = U_{Ca}\cos[\omega_r(t-t_0)] \quad (2)$$

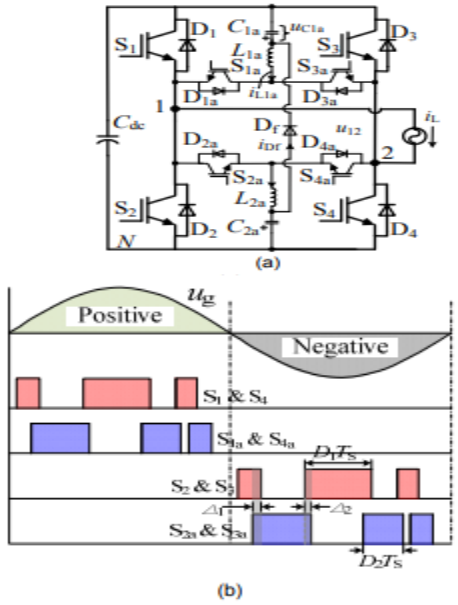

Fig. 7. Simplified SLF-HERIC. (a) Main circuit. (b) Driving logic at the grid frequency scale.

Stage 2 [t1, t2]: Refer to Fig. 6(b). At t1, anti-parallel diodes D1 and D4 are forward biased, and then the currents iS1 and iS4 flow through D1 and D4, respectively. Therefore, the ZCS turn-off condition of S1 and S4 is created. Resonant inductor currents iL1a and iL2a continually increase until they reach the peak current ILa at t2; at the same time, resonant capacitor voltages uC1a and uC2a continually reduce until they resonate to zero at t2. At stage 1 and 2

Stage 3 [t2, t3]: Refer to Fig. 6(c). At t2, the currents through D1 and D4 rise to the peak amplitude, and then reverse to decrease until they equal zero at t3. Meanwhile, resonant currents iL1a and iL2a begin to decrease from peak value ILa, as well as resonant voltages uC1a and uC2a start to increase reversely from zero. In the interval [t1, t3], main switches S1 and S4 can be turned off under the zero-current condition. Stage 4 [t3, t4]: Refer to Fig. 6(d). At t3, resonant currents iL1a and iL2a fall to IL, and then are clamped at IL by the AC output current. As a result, resonant inductors and resonant capacitors stop resonating. However, resonant capacitors C1a and C2a are continually charged by constant current IL, and the dedicated operation mode is named as energy supplement mode in order to compensate for the circulation loss of the resonant activity. At t4, the amplitude of voltages uC1a and uC2a across the resonant capacitors increases to -0.5UPV. Stage 5 [t4, t5]: Refer to Fig. 6(e). At t4, the charging current of resonant capacitors decreases sharply to zero, which is transferred into freewheeling diode Df. The inverter goes into the freewheeling period. auxiliary switches S1a and S4a are involved in the freewheeling loop, which is an obvious difference from the freewheeling loop of HERIC. In addition, the stage synchronizes two resonance tanks. Stage 6 [t5, t6]: Refer to Fig. 6(f). At t5, main switches S1 and S4 are turned on, the currents through resonant inductors decrease at a constant slope from IL. At the same time, the currents through S1 and S4 increase with same slope from zero. As a result, the ZCS turn-on condition of S1 and S4 is achieved. In addition, the falling rate of the resonant inductor current is controlled by the input DC voltage, as well as the current through resonant inductors and freewheeling diodes falls to zero at t6. The ZCS turn-off conditions of the auxiliary switches S5a and S6a and the freewheeling diodes Df are achieved at the end of this stage. Therefore, the reverse recovery problem is avoided Stage 7 [t6, t7]: Refer to Fig. 6(g). At t6, the current across main switches S1 and S4 rises to IL, and diodes D1a and D4a are forward biased. In order to reset the resonance, two resonance tanks begin to resonate again independently. The currents through resonant inductors L1a and L2a start to increase from zero until they equal the peak value -ILa at t7. At the same time, the voltages across resonant capacitors C1a and C2a begin to decrease from the negative peak voltage -UCa until they are equal to zero at t7. Stage 8 [t7, t8]: Refer to Fig. 6(h). At t7, resonant inductor currents iL1a and iL2a start to decrease from -ILa until they equal zero at t8. Meanwhile, resonant capacitor voltages uC1a and uC2a increase continually from zero until they rise to 0.5UPV. At t8, two resonance tanks stop resonating. In the interval [t6, t8], auxiliary switches S1a and S4a can be turned off under the zero-current condition. Stage 9[t8, t9]: Refer to Fig. 6(i), the inverter works at the normal power handling stage again. At t9, the inverter goes back to Stage 1 and starts a new switching cycle.

V. SIMULATION RESULTS AND DISCUSSIONS

In order to verify the effectiveness of the main contributions of this paper, a universal 3 kW prototype with the topologies shown in Fig. 4 has been built and tested. It is worth mentioning that the different topologies' experiments are able to test on the same hardware platform one by one, just need to change the wire connections between switches according to the topologies' structure. The main parameters and components are listed here. UPV: 360-400VDC; ug: 180-240 VRMS / 50 Hz; switching frequency fs: 50 kHz; Cdc1, Cdc2: 3×470 μF/350 VDC; L1, L2: 0.5 mH; C1: 2 μF; main switches S1-S4 are IKW40N60T from Infineon corporate; resonant switches S1a-S4a are IKW40N120T2 from Infineon with 1200 rated voltage due to the ringing between the resonant inductor and the parasitic capacitor of the resonant switch; Df1 are Df2 are RHRG5060 from Fairchild. Referring to the design criterions and steps of resonant parameters' calculation in literature [29] for the details, the resonant parameters Lr=8μF and Cr=120 nF are obtained. In the fabrication of the prototype, two EI33 magnetic cores are employed for making resonant inductors, and each winding is 12 turns; twelve 10 nF / 400 V film capacitors are connected in parallel for each resonant capacitor to better load the pulse current. Finally, the photograph of the prototype with SLF-H6-II circuit is illustrated in Fig. 8. In the designed specifications, maximum IL=19.28 A, ILa=22.05 A, Tr=6.15μs, and the turn-on current rising rate of the main and auxiliary

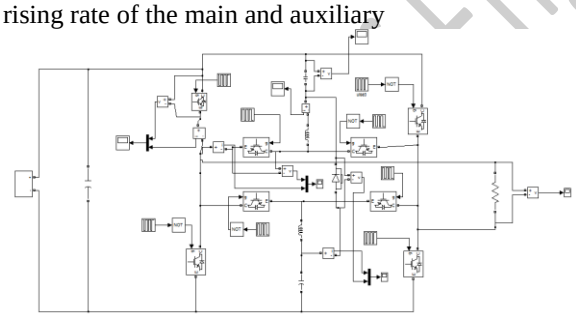

Fig8: Proposed simulation diagram

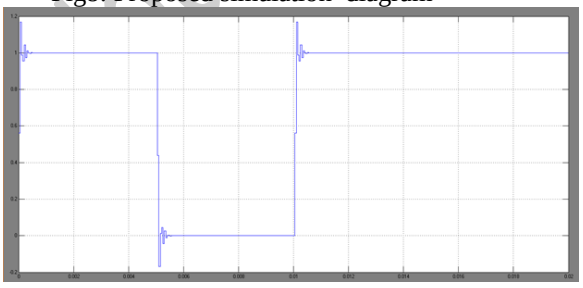

Fig9: Output voltage

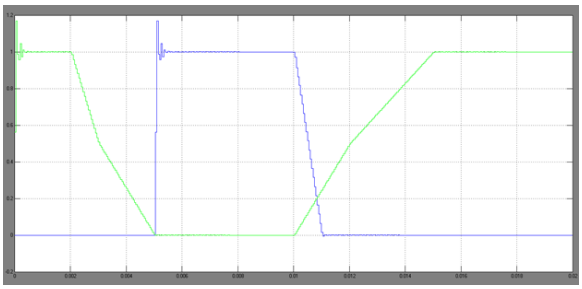

Fig10:Is1, Us1

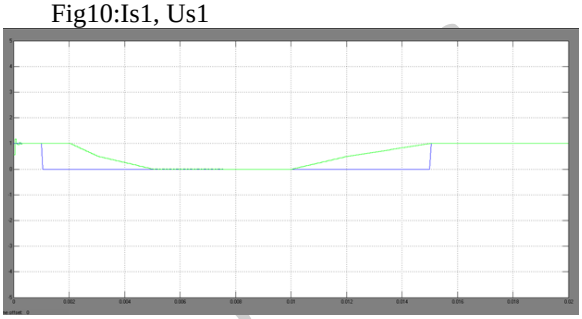

Fig11: Vda1, Vsa1

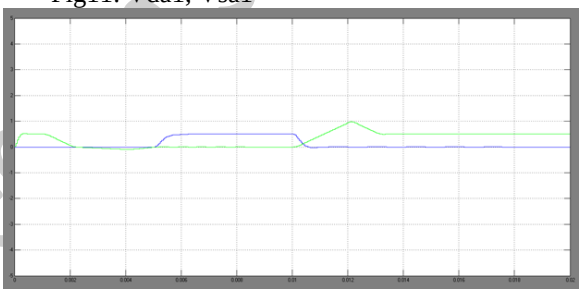

Fig12: Isa1, Vsa1

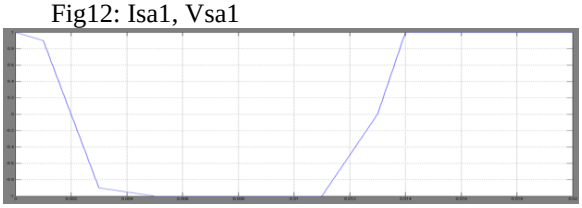

Fig13: Uc1a

VI. CONCLUSION

This paper has successfully developed a soft-switching configuration for transformerless photovoltaic grid-connected inverters, which is able to guide the creation of soft-switching TLIs. In order to prove the proposed soft-switching configuration, two basic resonance tanks fitting for the configuration have been proposed and used in HERIC, H5, H6-I and H6-II, respectively. As a result, the zero-current turn-on and turn-off of all power semiconductor devices are realized, and the switching loss-free (SLF) target has been implemented in full bridge type TLIs. Meanwhile, these advantages are proved based on a universal prototype platform. Therefore, the proposed SLF-TLIs are suitable for next generation high power density PV grid-connected inverter systems. It is worth noting that there is a voltage spike in the turn-

off transition of auxiliary switches, which has some negative influence on the voltage rating of power devices, especially in high input voltage applications. One the other hand, a defined amount of reactive power for grid-tied PV inverters of the power rating over 4.6 kVA (single phase)/13.8 kVA (three phase) has been required by the latest grid codes. Therefore, the SLF with full power factor is a scheduled task to extend the application range of SLF-TLIs in the future.

REFERENCES

[1] T. Yi, Y. Wenli, L. Poh Chiang, and F. Blaabjerg, "Highly reliable transformerless photovoltaic inverters with leakage current and pulsating power elimination," IEEE Trans. Ind. Electron., vol. 63, DOI 10.1109/TIE.2015.2477802, no. 2, pp. 1016-1026, Feb. 2016

[2] X. Guo, and X. Jia, "Hardware-based cascaded topology and modulation strategy with leakage current reduction for transformerless PV systems," IEEE Trans. Ind. Electron., vol. 62, DOI 10.1109/TIE.2016.2607163, no. 12, pp. 7823–7832, Dec. 2016.

[3] W. Li, Y. Gu, H. Luo, W. Cui, X. He, and C. Xia, "Topology review and derivation methodology of single-phase transformerless photovoltaic inverters for leakage current suppression," IEEE Trans. Ind. Electron., vol. 62, DOI 10.1109/TIE.2015.2399278, no. 7, pp. 4537-4551, July, 2015.

[4] X. Guo, "A novel CH5 inverter for single-phase transformerless photovoltaic system applications," IEEE Trans. Circuits and Systems II: Express Briefs, vol. 64, no. 10, pp. 1197-1201, 2017.

[5] H. Xiao, K. Lan, and L. Zhang, "A quasi-unipolar SPWM full-bridge transformerless PV grid-connected inverter with constant common-mode voltage," IEEE Trans. Power Electron., vol. 30, DOI 10.1109/ TPEL.2014.2331367, no. 6, pp. 3122–3132, Jun. 2015.

[6] L. Zhang, K. Sun, Y. Xing, and M. Xing, "H6 transformerless full-bridge PV grid-tied inverters," IEEE Trans. Power Electron., vol. 29, DOI 10.1109/TPEL.2013.2260178, no. 3, pp. 1229-1238, Mar. 2014.

[7] B. Gu, J. Dominic, J.-S. Lai, C.-L. Chen, T. LaBella, and B. Chen, "High reliability and efficiency single-phase transformerless inverter for grid-connected photovoltaic systems," IEEE Trans. Power Electron., vol. 28, DOI 10.1109/TPEL.2012.2214237, no. 5, pp. 2235-2245, May 2013.

[8] E. Koutroulis and F. Blaabjerg, "Design optimization of transformerless grid-connected PV inverters including reliability," IEEE Trans. Power Electron., vol. 28, DOI 10.1109/TPEL.2012.2198670, no. 1, pp. 325-335, Jan. 2013.

[9] S. Heribert, S. Christoph, and K. Jurgen, "Inverter for transforming a DC voltage into an AC current or an AC voltage," Europe Patent 1 369 985 (A2), 2003.

[10] M. Victor, F. Greizer, S. Bremicker, and U. Hubler, "Method of converting a direct current voltage from a source of direct current voltage, more specifically from a photovoltaic source of direct current voltage, into a alternating current voltage ," U. S. Patent 7 411 802 B2, 2008.

AUTHOR'S DETAILS:

N.AHMED HUSSAIN
I Completed My B.Tech in Vignana Bharati Institute of science and technology, Affiliated to JNTUA Ananthapuramu.Now he is pursing M.Tech in Power Electronics from Tadipatri Engineering College ,Affiliated to JNTUA Ananthapuramu,Andharapradesh.Area of interest Power Electronics.
Email Id:ahmedengineer14969@gmail.com

S.SASIDHAR REDDY
Received the Master of Technology in Electrical Power System from SIR C. V RAMAN INSTITUTE OF TECHNOLOGY AND SCIENCE ,Affiliated to JNTUA ,Ananthapuramu.B.Tech Degree from SRI KOTTAM TULASIREDDY Memorial college,Affiliatedto JNTUH , Hyderabad. Currently he is working as Asst.Professor in Tadipatri Engneering College in department of Electrical Electronics Engneering ,Tadipatri ,Ananthapuramu ,Andharapradesh.Area of interest Power Electronics.
Email Id:sasidharreddy03@gmail.com

Vol 11, Issue 3, MARCH /2020
ISSN NO:0377-9254

M.NAVEEN BABU

Received the Master Of Technology in Elecrical Power System from Sri KrishnadevarayaEngneeringCollege ,Gooty,JNTUAUniversity,Ananthapuramu. B.Tech Degree from Madanapalle Institute Of Technology & Science ,Affiliated to JNTUA , Ananthapuramu.Currently he is working as Asst.Professor & HOD in TadipatriEngneering College in department of Electrical Electronics Engneering , Tadipatri ,Ananthapuramu ,Andharapradesh.Area of interest Electrical Machines, Power System.

Email Id:naveenbabumidde@gmail.com